Journal of Asian Ceramic Societies 2 (2014) 68–76

Contents lists available at ScienceDirect

Journal of Asian Ceramic Societies

journal homepage: www.elsevier.com/locate/jascer

Synthesis of $BaTiO_3$ nanoparticles from TiO_2-coated $BaCO_3$ particles derived using a wet-chemical method

Yuuki Mochizuki [a,*], Naoto Tsubouchi [b], Katsuyasu Sugawara [a]

[a] Faculty of Engineering and Resources Science, Akita University, Akita 010-8502, Japan
[b] Center for Advanced Research of Energy and Materials, Faculty of Engineering, Hokkaido University, Sapporo 060-8628, Japan

ARTICLE INFO

Article history:
Received 18 November 2013
Received in revised form 10 January 2014
Accepted 15 January 2014
Available online 6 February 2014

Keywords:
Barium titanate
Barium carbonate
Amorphous titania
Coating
Calcination

ABSTRACT

$BaCO_3$ particles coated with amorphous TiO_2 precursor are prepared by a wet chemical method to produce $BaTiO_3$ nanoparticles at low temperatures. Subsequently, we investigate the formation behavior of $BaTiO_3$ particles and the particle growth behavior when the precursor is subjected to heat treatment. The state of the amorphous TiO_2 coating on the surface of $BaCO_3$ particles depends on the concentration of NH_4HCO_3, and the optimum concentration is found to be in the range 0.5–1.0 M. Thermogravimetric curves of the $BaCO_3$ particles coated with the TiO_2 precursor, prepared from $BaCO_3$ particles of various sizes, show $BaTiO_3$ formation occurring mainly at 550–650 °C in the case of fine $BaCO_3$ particles. However, as evidenced from the curves, the temperature of formation of $BaTiO_3$ shifts to higher values with an increase in the size of the $BaCO_3$ particles. The average particle size of single phase $BaTiO_3$ at heat-treatment temperature of 650–900 °C is observed to be in the range 60–250 nm.

1. Introduction

Barium titanate ($BaTiO_3$), with its Perovskite-type crystal structure, has been applied as a dielectric material in multiple-layer ceramic condensers (MLCCs), as a resistive element in positive temperature coefficient (PTC) thermistors and as an insulating phase in devices exhibiting inorganic electroluminescence (EL). In the last decade, miniaturization of electronic parts has been necessitated by advancements in information technology [1,2]. In particular, miniaturization and high capacity of MLCCs have been progressed. Such high capacitive decoupling abilities and miniaturization can be accomplished by lamellation of the dielectric layer and by increasing the number of laminations. In recently, MLCCs having dielectric thickness of 0.5 μm produced by Murata Manufacturing Co. Ltd. [3], and it is expected that the thickness of the capacitor layer will be reduced further. Therefore, fine $BaTiO_3$ particles with nano-sizes are much sought after.

Preparation of $BaTiO_3$ has conventionally been performed using solid-state [4–12], oxalic acid-based [13], citric acid-based [14], alkoxide-based [15], sol–gel [16] and hydrothermal [17–19] methods. In particular, solid-state reaction is one of the most commonly used synthetic methods for fabricating pure $BaTiO_3$ particles; however, high calcination temperatures are required to obtain pure $BaTiO_3$ phase by this method. Further, the particles obtained are usually coarse and agglomerated, because the particle growth increases with increasing calcination temperature. According to previous studies [7,8], the solid-state reaction between $BaCO_3$ and TiO_2 first forms $BaTiO_3$ layers on the TiO_2 particle surface, owing to the reaction between the contacting interfacial surfaces of $BaCO_3$ and TiO_2, followed by the diffusion of Ba or O ions into the TiO_2 particles. To clarify the solid-state reaction process and to understand the effects of temperature on the structure and formation of $BaTiO_3$, Raman spectroscopy and X-ray diffraction (XRD) analysis were performed on TiO_2 (4 μm)–$BaCO_3$ core–shell particles (TiO_2 particles coated with $BaCO_3$ particles) [20–22]. While using TiO_2–$BaCO_3$ core–shell particles, intermediates such as $BaTi_5O_{11}$, $BaTi_4O_9$, $BaTi_2O_5$ and Ba_2TiO_4 were observed during calcination, and temperatures above 1100 °C were required to produce single-phase $BaTiO_3$. The process of $BaTiO_3$ formation by calcination of TiO_2 (S_{BET} = 10 m^2/g)–$BaCO_3$ (100–150 nm) core–shell particles prepared by homogeneous precipitation was investigated using XRD and thermogravimetry (TG) [23,24]. Thermogravimetric changes started above 600 °C, and the weight loss was completed at 1000 °C via the formation of an intermediate

* Corresponding author. Present address: Center for Advanced Research of Energy and Materials, Faculty of Engineering, Hokkaido University, Sapporo 060-8628, Japan. Tel.: +81 11 706 6848; fax: +81 11 726 0731.
E-mail address: mochi@eng.hokudai.ac.jp (Y. Mochizuki).

Peer review under responsibility of The Ceramic Society of Japan and the Korean Ceramic Society.

Production and hosting by Elsevier

2187-0764 © 2014 The Ceramic Society of Japan and the Korean Ceramic Society. Production and hosting by Elsevier B.V. All rights reserved.
http://dx.doi.org/10.1016/j.jascer.2014.01.007

Ba_2TiO_4 species at around 900 °C. The final average particle size of $BaTiO_3$ was 420–560 nm, which were formed from agglomeration of primary particles 150–200 nm in size [24]. As is well known, particle growth of $BaTiO_3$ during the solid-state reaction between $BaCO_3$ and TiO_2 depends on the particle size of the parent TiO_2 [25]. During calcination of TiO_2 (50 nm) or $BaCO_3$ (49 nm), the average particle sizes increase to 60 and 150 nm, respectively, upon calcination at 600 °C, and 75 and 370 nm, respectively, at 700 °C [26]. To obtain fine $BaTiO_3$ particles, it is thus very important to inhibit mutual contact of $BaCO_3$ particles, and to ensure that the reaction between $BaCO_3$ and TiO_2 occurs at lower temperatures. Given these requirements, the analysis of $BaTiO_3$ produced from $BaCO_3$–TiO_2 core–shell particles, prepared by the precipitation method using peroxo-titanium(IV) solution, was proposed [27–29]. It has been found from the differential thermogravimetric curve of $BaCO_3$ (S_{BET} = 31 m^2/g)–TiO_2 core–shell particles that $BaTiO_3$ formation occurs in one step at temperatures in the range of 600–650 °C, while secondary particles as large as 100–150 nm form by agglomeration of 20–50 nm-sized primary particles of at 700 °C with a treatment time of 1 h [27]. However, the thermogravimetric change in $BaCO_3$ (S_{BET} = 3.3 m^2/g)–TiO_2 core–shell particles was observed to proceed in three-steps at 800 °C with a treatment time of 8 h, resulting in hollow $BaTiO_3$ particles [28]. In addition, the agglomeration of 100–200 nm $BaTiO_3$ particles occurs at 900–1000 °C without the formation of intermediate. From these reports, it is evident that TiO_2-coated $BaCO_3$ particles are more effective than $BaCO_3$-coated TiO_2 particles to obtain fine $BaTiO_3$ particles at lower temperature ranges. However, the precipitation of TiO_2-coated $BaCO_3$ particles by previously reported methods make use of hydrogen peroxide, a substance that compromises the cost-effectiveness and the safety of the process.

In this present work, to obtain fine $BaTiO_3$ particles at lower temperatures by solid-state reaction, firstly, the conditions for the preparation of $BaCO_3$ particles coated with TiO_2 by a wet-chemical method were optimized. Further, $BaTiO_3$ formation as a function of heat treatment temperature was studied.

2. Experimental

2.1. Materials

$BaCO_3$ samples used in this study were received from Solvay Bario e Derivati, Massa, Italy. These samples shall henceforth be referred to as A (S_{BET} = 3.2 m^2/g, $d_{av.}$ = 437 nm, needles), B (S_{BET} = 12.2 m^2/g, $d_{av.}$ = 115 nm, needles) and C (S_{BET} = 28.5 m^2/g, $d_{av.}$ = 49 nm, needles). In addition, commercial $BaCO_3$ (S_{BET} = 3.3 m^2/g, $d_{av.}$ = 424 nm) (NACALAI TESQUE, G.R.), was also used. $TiCl_4$ solution, which was used as the Ti source, was prepared by adding $TiCl_4$ (NACALAI TESQUE, C.P.) dropwise to a 2 M solution of HCl in distilled water kept in an ice bath, along with constant stirring.

2.2. Preparation of TiO_2-coated $BaCO_3$ particles

The preparation of $BaCO_3$ particles coated with TiO_2 was performed using the apparatus shown in Fig. 1. First, a predetermined amount of NH_4HCO_3 (NACALAI TESQUE, G.R.) was dissolved in 100 mL of distilled water. $BaCO_3$ was dispersed in the NH_4HCO_3 solution and ultrasonicated for 15 min at room temperature. Then, the prepared $TiCl_4$ solution, equivalent to the amount of added $BaCO_3$ (Ba/Ti = 1 (molar ratio)), was injected into the $BaCO_3$–NH_4HCO_3 solution through a micro tube track at the rate of 0.2 mL/min, even as the solution was stirred at 500 rpm at room temperature. After the addition of the $TiCl_4$ solution, the reaction

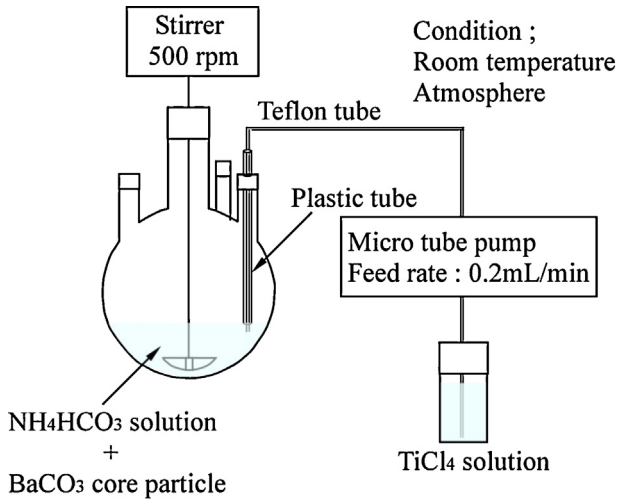

Fig. 1. Experimental apparatus used for the preparation of TOP-BC particles.

product ($BaCO_3$ particles coated with TiO_2 precursor particles) was recovered by filtration, and dried at 107 °C for 12 h in air.

Then, the prepared TiO_2 precursor-coated $BaCO_3$ particles were heated at 10 °C/min to a predetermined temperature (400–1000 °C) in ambient atmosphere. The heat-treated samples were characterized using powder XRD (RIGAKU, RAD-PC SYSTEM) analysis. After crushing, the samples were loaded into glass holders for the XRD measurement. Cu-Kα radiation was used at generator settings of 30 kV and 20 mA. The XRD patterns were collected in the 2θ range of 3–80° at a speed of 4°/min with a scan step of 0.02°. The tetragonality of $BaTiO_3$ obtained by heat treatment was evaluated using the *c*/*a* ratio from the lattice constants along the "*c*" and "*a*" axes of the $BaTiO_3$ crystal lattices. The lattice constants "*c*" and "*a*" were determined by using an internal standard method involving Si addition. The *c*/*a* values were calculated using the lattice constant calculation program [30].

TG analysis was performed by using a differential TG analyzer (BRUKER, TAS-2000), and the morphologies of the samples were observed with a scanning electron microscope (SEM) (JOEL, JSM-6510LV). The specific surface area of the samples was measured with a specific surface area analyzer (YUASA IONICS, NOVA1200), and the amount of $BaTiO_3$ formed with the heat treatment temperature was quantified based on the procedure reported in Ref. [31].

Henceforth, $BaCO_3$ particles (BC) coated with TiO_2 precursor particles (TOP) and the product obtained after heat treatment up to a predetermined temperature will be denoted as BC-TOP and BC-TO, respectively.

3. Results and discussion

3.1. Effect of NH_4HCO_3 concentration on the preparation of BC-TOP

Fig. 2 shows the effect of the concentration of NH_4HCO_3 solution used during the preparation of the BC-TOP particles. Sample C was selected for this investigation. The yield of BC-TOP particles was constant above 0.5 M NH_4HCO_3. Fig. 2 shows the variation of pH and weight of the product as a function of NH_4HCO_3 concentration observed during the preparation of BC-TOP and TOP. The gradation in weight change of BC-TOP corresponded to that of TOP. The pH after the reaction was constant at 8.5 above NH_4HCO_3 concentrations of 0.5 M. At lower NH_4HCO_3 concentrations (<0.5 M), $BaCO_3$ can be expected to be dissolved by the addition of the $TiCl_4$ solution,

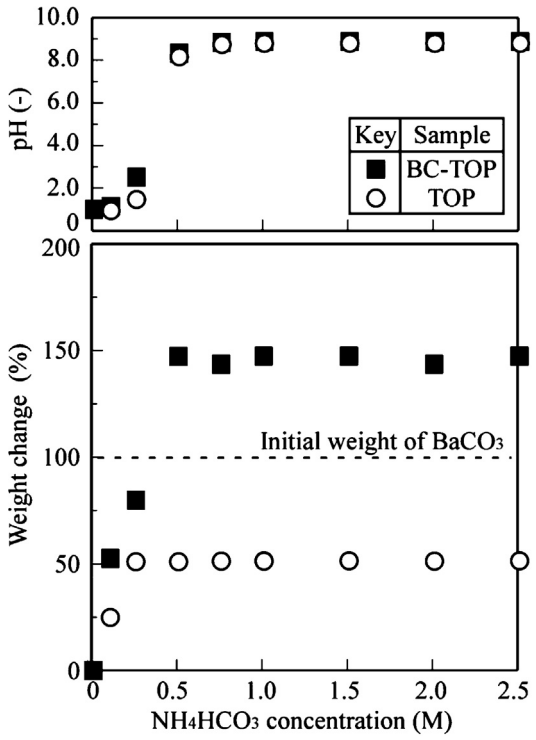

Fig. 2. Changes in pH and product weight as a function of the NH_4HCO_3 concentration used in the preparation of BC-TOP. (Sample C was used as the $BaCO_3$ starting material.)

which is highly acidic, because the weight of BC-TOP produced was lower than the initial weight of $BaCO_3$. The coating reactions between $TiCl_4$ and NH_4HCO_3 solutions are reported to be as follows [32,33]:

$$HCO^{3-} + H_2O \rightarrow H_2CO_3 + OH^- \quad \text{(in acidic solution)} \tag{1}$$

$$H_2CO_3 \rightarrow H_2O + CO_2(g) \tag{2}$$

$$Ti_n{}^+ + nOH^- \rightarrow Ti(OH)_n{\cdot}H_2O(s) \tag{3}$$

$$NH_4HCO_3 + TiCl_4 \rightarrow Ti(OH)_n{\cdot}H_2O(s) + NH_4Cl(l) + H_2O(l) + CO_2(g) \quad \text{(Total reaction)} \tag{4}$$

During the reaction, chlorine ion reacts with $NH_4{}^+$ ion and remains in solution as NH_4Cl (l). According previous work, the difference of surface potential between two solid phases is importance for the formation of the coating [27]. At pH window 6–10, the zeta potential of $BaCO_3$ is positive, while that of TiO_2 is negative. Therefore, NH_4HCO_3 concentration of ≥0.5 M may be suitable for preparation of BC-TOP, because the pH after the reaction was constant at 8.5.

Fig. 3 illustrates the effect of the concentration of NH_4HCO_3 on the DTG curves of TOP and BC-TOP. TOP particles obtained without NH_4HCO_3 exhibited a main peak at around 100 °C. Fig. 3 also shows the DTG peaks for the products prepared with solutions of NH_4HCO_3 concentrations <0.5 M. The DTG curves of BC-TOP obtained below 0.5 M were similar with that of TOP. The XRD profiles of the products obtained using 0–0.25 M NH_4HCO_3 solutions gave broad amorphous patterns, and no peaks of $BaCO_3$ were detected. However, peaks attributable to $BaCO_3$ were observed in the products obtained using 0.5 M NH_4HCO_3 solutions. These results indicate that $BaCO_3$ was dissolved by $TiCl_4$ in NH_4HCO_3 solutions with concentrations ranging from 0 to 0.25 M, and the main product obtained was TOP. The main peaks of the DTG curves of the products obtained using NH_4HCO_3 solutions with concentrations ≥0.5 M were observed at around 600 °C. However, the DTG peaks around 800 °C increased with increasing NH_4HCO_3 solution concentration. It has been previously reported that the DTG peak at amount 800 °C is caused by the rate limiting diffusion of Ba ions into TiO_2 particles during the solid-state reaction between $BaCO_3$ and TiO_2 [7,8]. Therefore, higher concentrations of NH_4HCO_3 might lead to heterogeneous TOP coating on $BaCO_3$ particles or products of coarse TOP particles. The coating proceeds by the growth of the homogeneous-nuclei, produced by the impact or adherence between core particles [32]. In the case of higher NH_4HCO_3 concentrations, coarse particles can be expected to be formed owing to agglomeration among core particles due to stirring. This agglomeration is the result of the hydrolysis reaction that occurs around the region of added $TiCl_4$. Therefore, the homogeneous TiO_2 precursor coating on $BaCO_3$ particle surface could not have formed under conditions of high NH_4HCO_3 concentrations. In the light of these results, 0.5 M NH_4HCO_3 solutions were used for the preparation of BC-TOP subsequently.

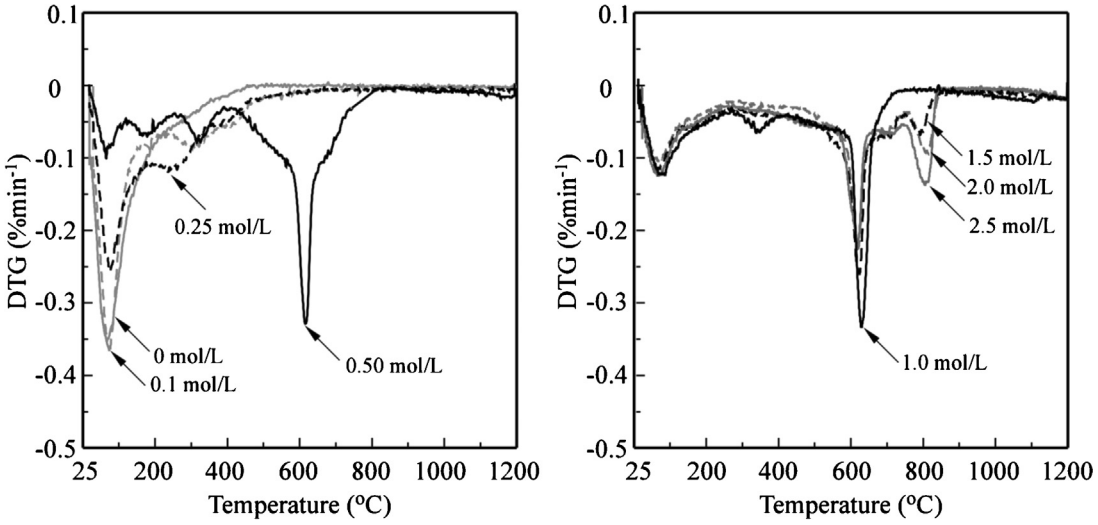

Fig. 3. Effect of NH_4HCO_3 concentrations on the DTG curves of TOP and BC-TOP. (Sample C was used as the $BaCO_3$ starting material.)

3.2. Morphology of BC-TOP particles

Fig. 4 shows the morphologies of the BC-TOP prepared using four kinds of $BaCO_3$ with different particle sizes. The smooth surfaces of the $BaCO_3$ particles were coated with fine TOP after the coating treatment. The agglomerated TOP observed by SEM was formed from <100 nm TOP generated during the preparation process without $BaCO_3$. These results indicate that the coating method used in the present study can be used to coat various particles of different sizes.

3.3. Effect of $BaCO_3$ particle size on the formation of $BaTiO_3$

Fig. 5(a) presents the DTG curves of mixtures of TOP and $BaCO_3$ (NT, A, B and C) prepared by physical mixing using triturator. The Ba/Ti molar ratio in physical mixtures was 1. When NT and A were used as $BaCO_3$ starting materials, two steps of weight loss were observed at 550–950 and at 950–1050 °C. However, the weight loss in B and C in three steps occurred at around 550–650, 750–900 and 900–1000 °C. The initial weight loss temperature for all physical mixtures of TOP and $BaCO_3$ was observed to be at around 550 °C, and the kinetics of weight loss, which increased in the order of NT < A < B < C, strongly depended on the $BaCO_3$ particle size. It is well known that the kinetics of $BaTiO_3$ formation depends on the size of TiO_2 particles [25]. Despite the TOP being fine, with sizes below 100 nm as seen in Fig. 4, the kinetics of $BaTiO_3$ formation of physical mixtures of TOP and $BaCO_3$ were very low; however, the reaction kinetic improved above 800 °C. This indicates that the dispersion of agglomerated TOP would not occur by mere physical grinding.

Fig. 5(b) represents the DTG curves of BC-TOP obtained from NT, A, B and C samples. The shoulder and main peaks in the case of samples A was observed around 700 and 850 °C, respectively. In the case of NT samples, the shoulder and main peaks were found at around 600, 700 and 850 °C. Although the main peak observed at 850 °C between BC-TOP and physical mixtures corresponded, the peak observed above 900 °C in the case of the physical mixtures was not observed in the case of the BC-TOP. In the case of BC-TOP

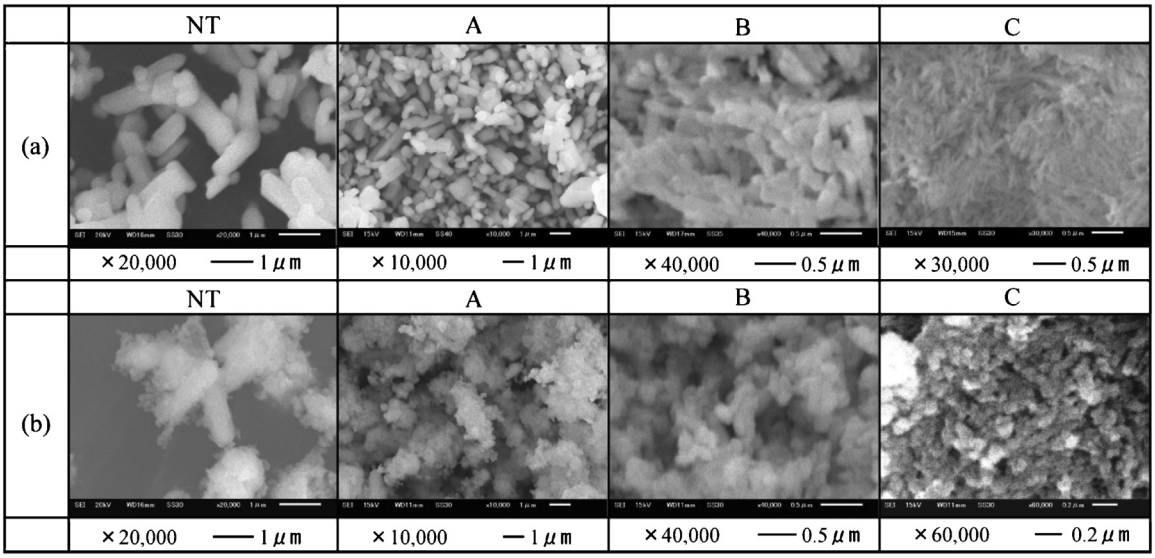

Fig. 4. Morphologies of BC (a) and BC-TOP (b).

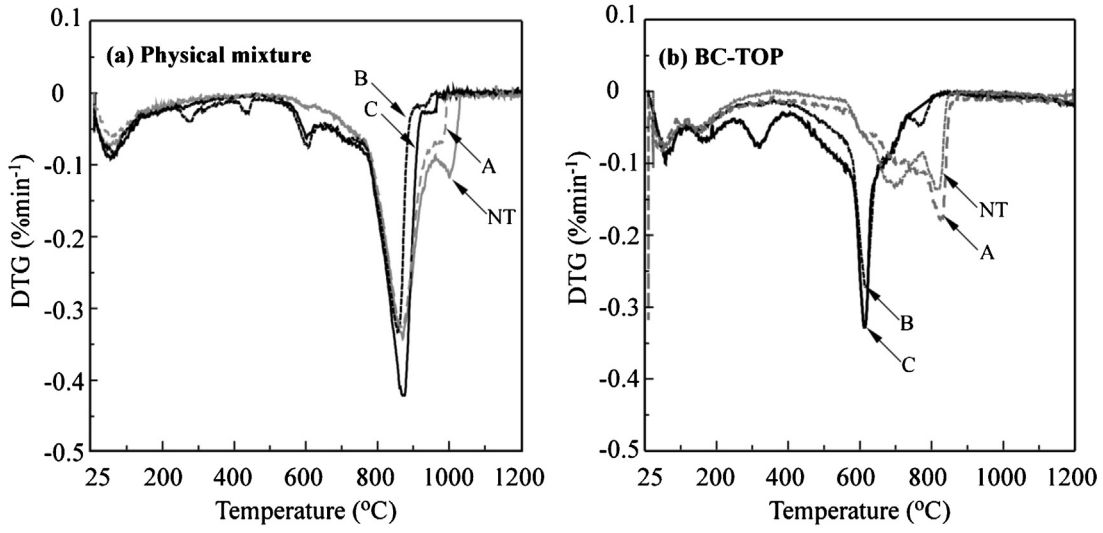

Fig. 5. DTG curves of physical mixtures of $BaCO_3$ and TiO_2 precursor (a) and BC-TOP (b).

obtained from samples B and C, the largest peak was observed at around 600 °C, and a small peak was also observed at a temperature in the range of 750–800 °C in the case of sample obtained from only B. Comparing the DTG curves obtained from BC-TOP and the physical mixture, the peak around 600 °C exhibited by the BC-TOP particles was large while the peak around 850–900 °C in the case of the physical mixture was not observed. In addition, the DTG curves obtained from BC-TOP and physical mixtures obtained from C, B and NT, A were all quite different. Hence, it can be concluded that smaller $BaCO_3$ particle sizes promoted $BaTiO_3$ formation at lower temperatures. According to a previous report, the intensity of the DTG peak at around 650 °C, corresponding to the solid-state reaction between TiO_2 (67 nm) and $BaCO_3$ (48 nm), is larger than the peak from between TiO_2 (67 nm) and $BaCO_3$ (136 or 655 nm) [5]. In the case of the solid-state reaction using $BaCO_3$ (54 nm)–TiO_2 (16 or 28 nm) or $BaCO_3$ (482 nm)–TiO_2 (16 nm), the extent of weight loss at around 660 °C is reported to strongly depend on the TiO_2 particle size [4]. The DTG curve profile obtained for $BaCO_3$ (54 nm)–TiO_2 (16 or 28 nm) [4] was similar to the DTG curve of BC-TOP obtained by using B and C. The formation of $BaTiO_3$ through the solid-state reaction between $BaCO_3$ and TiO_2 follows the following reaction scheme [8,34,35]:

$$BaCO_3 + TiO_2 \rightarrow BaTiO_3 + CO_2(g) \quad (5)$$

$$BaTiO_3 + BaCO_3 \rightarrow Ba_2TiO_4 + CO_2(g) \quad (6)$$

$$Ba_2TiO_4 + TiO_2 \rightarrow 2BaTiO_3 \quad (7)$$

In the first step of $BaTiO_3$ formation, the reaction between $BaCO_3$ and TiO_2 surface occurs at the particle contact interface (Eq. (5)), and the surface of the TiO_2 particle is coated with the $BaTiO_3$ formed. Then, Ba ions from the formed $BaTiO_3$ diffuse into TiO_2 particles in accordance with the reactions expressed in Eqs. (6) and (7). Eq. (5) will be dominant during heat treatment of BC-TOP obtained using B and C, as evident from the largest DTG peak observed at around 600 °C. However, in the case of BC-TOP obtained from A and NT, diffusion of Ba ions will be the rate limiting phenomenon, because these $BaCO_3$ particles are larger than those of B and C. It is possible that the starting temperatures of $BaTiO_3$ formation were shifted to a lower temperature region by the use of $BaCO_3$ particles coated with TOP of different sizes.

3.4. Formation behavior of $BaTiO_3$ from BC-TOP

Fig. 6 shows the behavior of $BaTiO_3$ formation as a function of the heat treatment temperature. In the case of samples obtained from B and C, which show the main DTG peaks around 600 °C as seen in Fig. 5, $BaTiO_3$ formation increased dramatically as the heat treatment temperatures increased from 500 to 700 °C. The extent of $BaTiO_3$ formation was 100% at 800 °C. Although the starting temperature of $BaTiO_3$ formation with samples obtained from B and C were similar, the formation kinetics of reaction with sample obtained from C was larger than that of the reaction with sample obtained from B. $BaTiO_3$ was produced above 550 °C in the case of sample obtained from A and NT, and these formation behaviors were also similar. The starting temperature of $BaTiO_3$ formation from samples obtained from B and C were lower than that of $BaTiO_3$ formation from samples obtained from A and NT. These results indicate that the kinetics of $BaTiO_3$ formation from the BC-TOP also depends on the particle size of $BaCO_3$.

3.5. Characterization of BC-TOP particles as a function of heat treatment temperature

Fig. 7(a)–(d) show the changes in the XRD profiles of BC-TOP with respect to the heat treatment temperature. The peaks

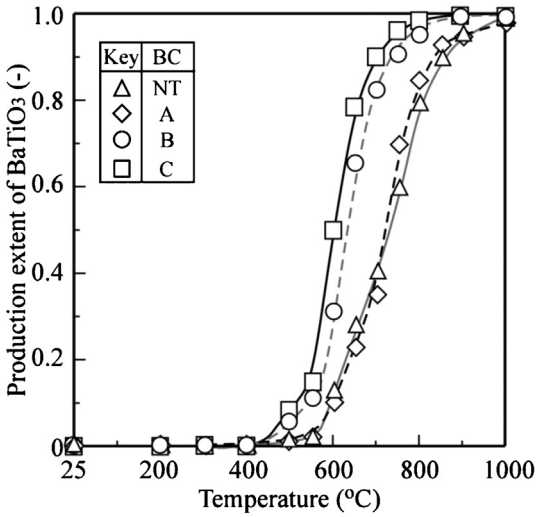

Fig. 6. Change in formation extent of $BaTiO_3$ from BC-TOP with temperature.

attributable to $BaTiO_3$ are observed at around 600 °C for all BC-TOP. In the case of samples obtained from B and C, the $BaCO_3$ peak intensities dramatically decreased at around 600–650 °C, whereas, the peak intensity of $BaTiO_3$ increased. In samples obtained from B and C, single-phase $BaTiO_3$ was observed at 700 and 800 °C, respectively. Although the peaks attributable to $BaTiO_3$ in the case of samples obtained from A and NT were measured at around 600 °C, a heat treatment temperature of 900 °C was required to obtain single-phase $BaTiO_3$.

Changes in the morphologies of BC-TOP obtained at heat treatment temperatures ranging from 500 to 1000 °C are shown in Fig. 8. The original shapes of the samples prepared from A and NT were maintained up to 500–600 °C (Fig. 8(a) and (b)), while hollow particles were observed in the range 700–800 °C. In the case of BC-TOP obtained from A and NT, the $BaTiO_3$ formation occurred at around 600 °C, as indicated by the $BaTiO_3$ formation behavior and the results of the XRD analysis shown in Figs. 6 and 7, respectively. Hence, the reaction shown in Eq. (5), which indicates the diffusion of Ba ions into the TiO_2 phase at the contact surface between $BaCO_3$ and TiO_2, proceeded, even while maintaining the original shapes. It was found that the proportion of hollow particles decreased with increasing heat-treatment temperature and the agglomeration of the primary particles occurred at ~1000 °C. Fig. 8(c) and (d) shows the change in the morphologies of samples obtained from B and C. The hollow particles were also observed in the case of samples obtained from B in the range 600–700 °C, as in the case of samples obtained from A and NT. In the case of samples obtained from C, it was difficult to observe hollow particles, because the original particles were very fine. The temperature at which the hollow particles begin to form from samples obtained from B was 100 °C lower than the observed temperature in the case of samples obtained from A and NT. The diffusion of Ba ions into TiO_2 particles was estimated to occur at 600 °C for samples obtained from A. Previous reports suggest that the hollow structure can be maintained in the form of $BaCO_3$–TiO_2 core–shell particle up to 700 °C, because CO_2 generated from $BaCO_3$ decomposition during the solid-state reaction at temperatures up to 700 °C can move out of the shell through a small pore or crack in the TiO_2/$BaTiO_3$ phase; however, the hollow structure collapsed at 900 °C [27,28]. It has been proposed that during the sintering of the formed $BaTiO_3$ phase, CO_2 evolution increases with increasing heat-treatment temperature, and the partial pressure of CO_2 contributes to the collapse of the hollow particles to form fine spherical particles [27,28]. This may be a reason which

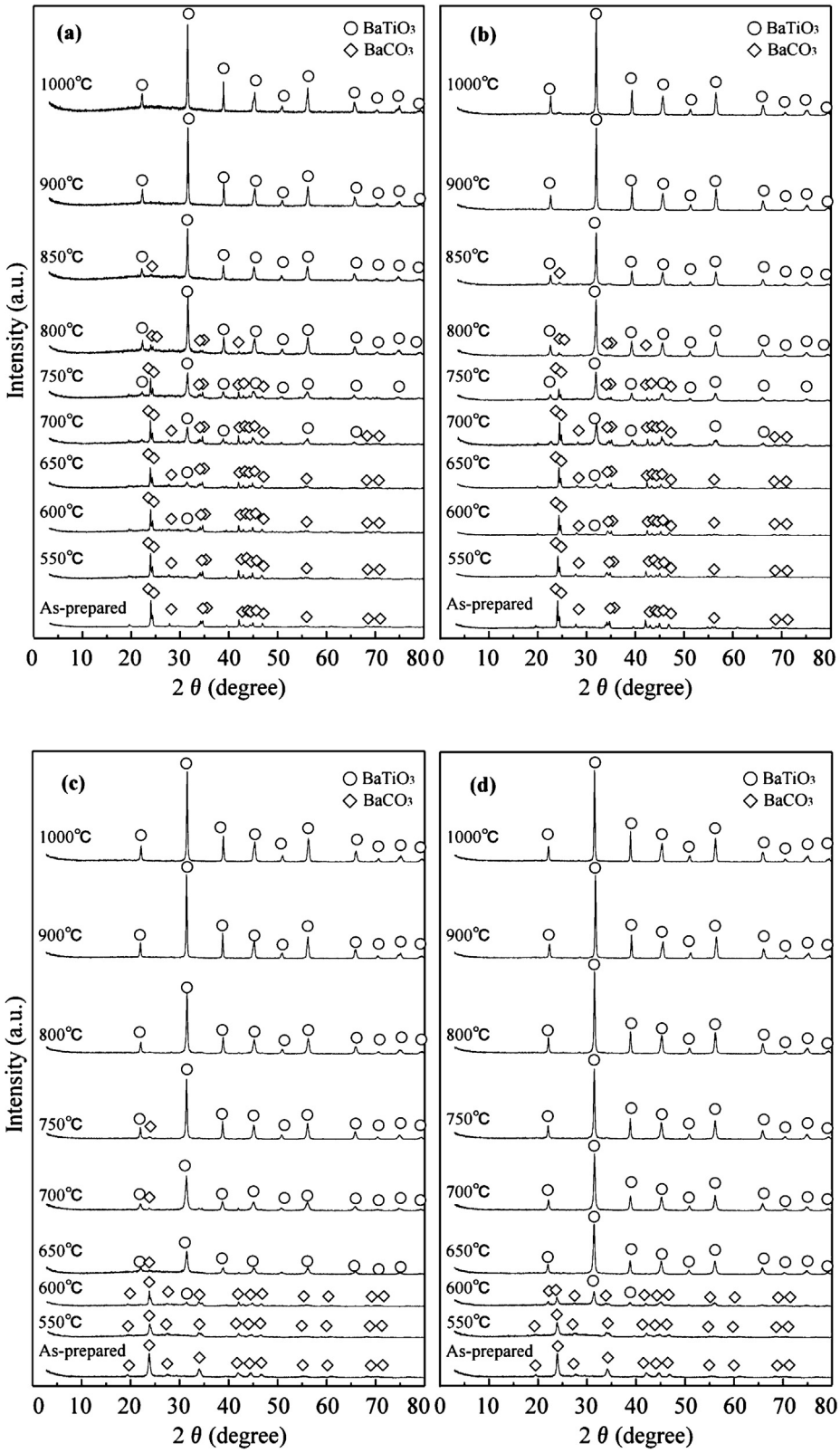

Fig. 7. Changes in XRD profiles of BC-TOP particles with temperature for samples obtained from NT (a), A (b), B (c) and C (d).

spherical $BaTiO_3$ particles formed from a needle BC. The collapse of the hollow particle was observed to occur around 700 °C in the present study, which is lower than the temperature reported in the previous study [27,28]. This collapse may occur even during sample preparation for SEM observation, because the hollow particles may be delicate.

Fig. 9 shows the gradation in the specific surface area of BC-TOP as a function of the heat treatment temperature. The specific

surface area at the starting temperature of $BaTiO_3$ formation (600 °C) for samples obtained from A and NT were 12–15 m^2/g; these values decreased with an increase in temperature. At 900 °C, at which single-phase $BaTiO_3$ was observed, the values of samples obtained from A and NT were 4 and 6 m^2/g, respectively. The specific surface areas of sample obtained from B (22 m^2/g) and C (25 m^2/g) observed at 600 °C decreased to around 16 and 14 m^2/g at 650 and 800 °C, respectively.

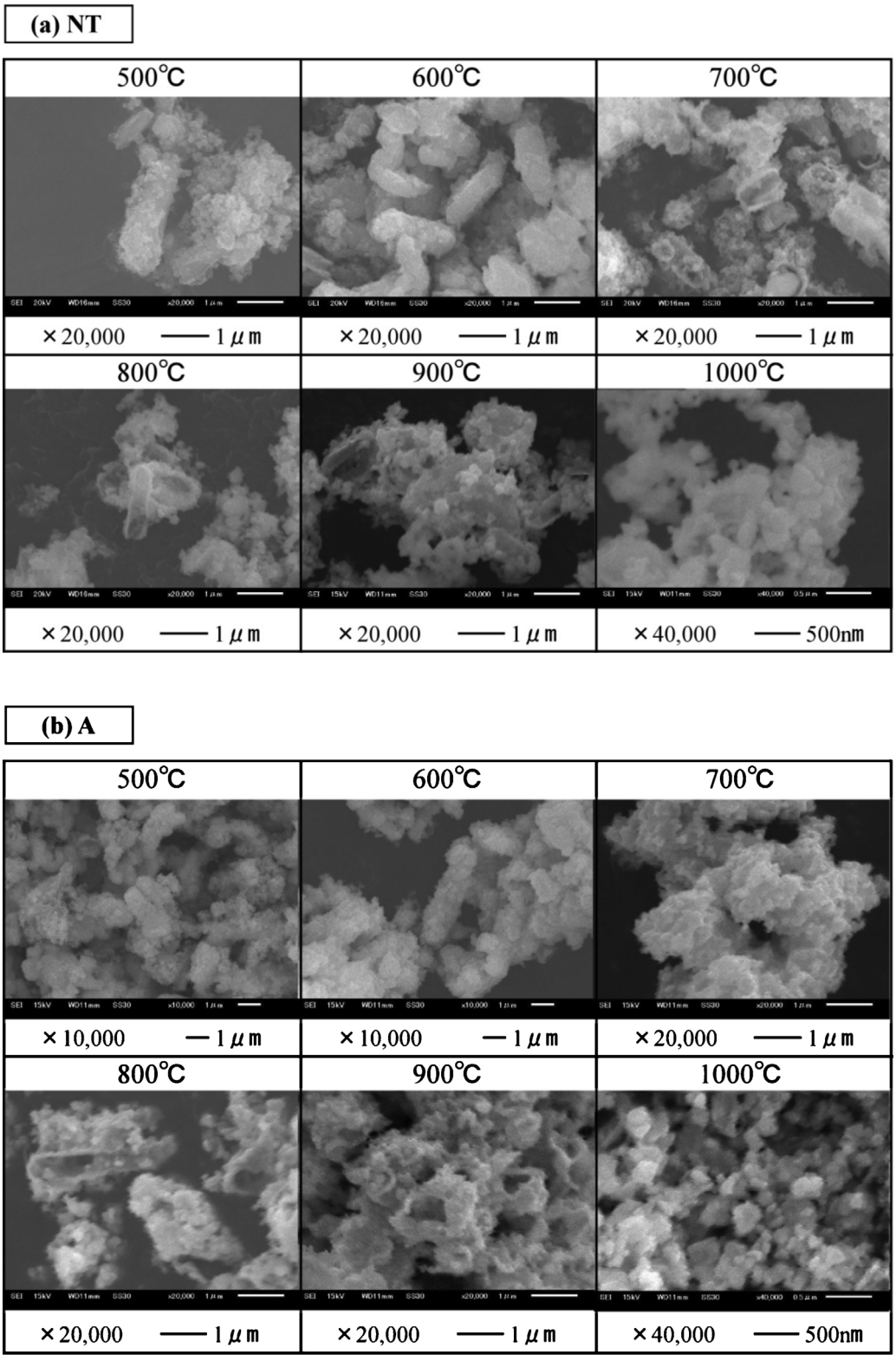

Fig. 8. Changes in morphologies of BC-TOP particles with temperature for samples obtained from NT (a), A (b), B (c) and C (d).

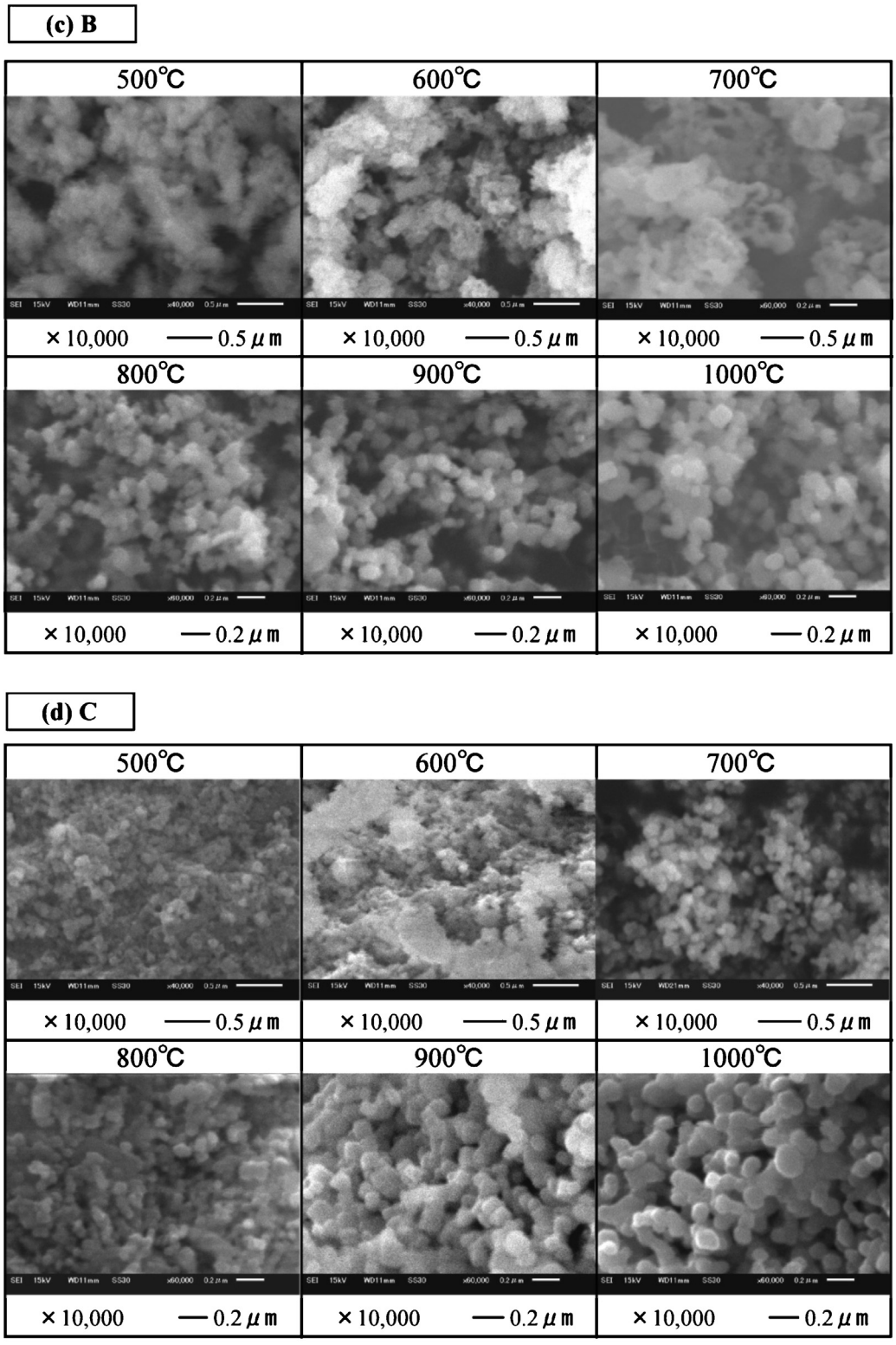

Fig. 8. (*Continued*).

Table 1 summarizes the particle size and the tetragonality, i.e., the *c*/*a* values, of $BaTiO_3$. The average particle size was calculated according to Eq. (9):

$$d_{av.} = 6/(\rho \times S) \quad (9)$$

where $d_{av.}$ is the average particle size of $BaTiO_3$ obtained at each temperature (nm), ρ is the density of $BaTiO_3$ (g/cm^3) and S is the specific surface area (m^2/g). In the case of samples obtained from NT and A, the average particle sizes of the $BaTiO_3$ particles at 900 °C, at which single phase $BaTiO_3$ was observed, were 250 and 155 nm, respectively. The corresponding *c*/*a* values were 1.002 and 1.003,

Table 1
Tetragonality (c/a) and average particle sizes of various samples treated at different temperatures.

Temperature (°C)	NT		A		B		C	
	c/a (–)	Particle size (nm)	c/a (–)	Particle size (nm)	c/a (–)	Particle size (nm)	c/a (–)	Particle size (nm)
650	–	–	–	–	–	–	1.002	60
700	–	–	–	–	–	–	1.002	65
750	–	–	–	–	1.003	75	1.004	70
800	–	–	–	–	1.006	80	1.006	75
900	1.002	250	1.003	155	1.006	130	1.007	120
1000	1.004	330	1.003	220	1.007	185	1.007	140

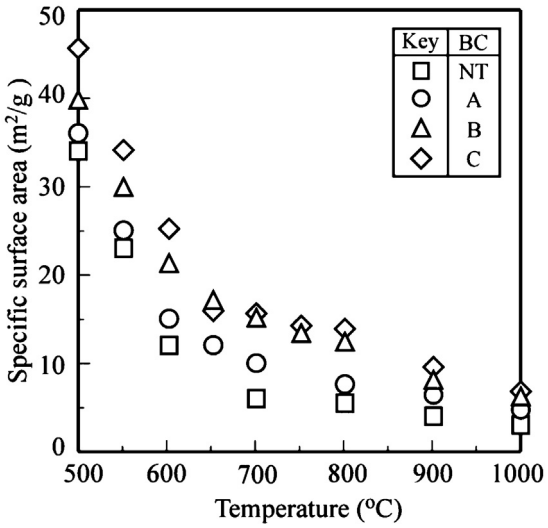

Fig. 9. Change in the specific surface area of BC-TOP with temperature.

respectively. However, the average particle size of 75 nm and c/a of 1.003 were estimated at 750 °C for samples obtained from B. For samples obtained from C, the corresponding average particle size and c/a values were 60 nm and 1.002, respectively. These values increased with increase in temperature. In the case of sample obtained from B and C, the average particle sizes dramatically increased above 800 °C, because the sizes depended on the agglomeration of $BaTiO_3$, as can be seen from the SEM observations. These results indicate that the preparation of $BaTiO_3$ with an average particle size of 60–250 nm and c/a of 1.002–1.007 was possible by using the method proposed in the present work.

4. Conclusions

In this work, to obtain fine $BaTiO_3$ particles at lower temperatures by the solid-state reaction, first, conditions for the preparation of $BaCO_3$ coated with TiO_2 particles by the wet-chemical method were optimized. Further, the behavior of $BaTiO_3$ formation was investigated.

The principal conclusions can be summarized as follows:

1. The preparation of $BaCO_3$ particles coated with TiO_2 precursors depends on the concentration of the NH_4HCO_3 solution used for its synthesis; the optimum concentration is in the range of 0.5–1.0 M.
2. $BaCO_3$ particles coated with TiO_2 precursor were formed from primary particles of amorphous TiO_2 of size <100 nm.
3. From the results of DTG and XRD analyses, it is evident that the fine $BaCO_3$ particles coated with TiO_2 precursor transformed into $BaTiO_3$ at 550–650 °C, while the larger particles formed $BaTiO_3$ at 900 °C.
4. The formation of $BaTiO_3$ from all types of $BaCO_3$ particles coated with TiO_2 precursors, prepared by the wet chemical method considered in the present work, was complete at temperatures lower than that of the solid-state reaction.
5. The average particle size at the temperature at which the single-phase $BaTiO_3$ was observed ranged from 60 to 250 nm.

References

[1] C. Pithan, D. Hennings and R. Waser, Int. J. Appl. Ceram. Technol., 2, 1–14 (2005).
[2] T. Yamamoto, Recent Technologies and Applications of Multilayered Ceramic Devices, CMC Publication, Japan (2006).
[3] http://www.murata.co.jp/
[4] M.T. Buscaglia, M. Bassoli, V. Buscaglia and R. Vormberg, J. Am. Ceram. Soc., 91, 2862–2869 (2008).
[5] M.T. Buscaglia, M. Bassoli, V. Buscaglia and R. Alessio, J. Am. Ceram. Soc., 88, 2374–2379 (2005).
[6] U. Manzoor and D.K. Kim, J. Mater. Sci. Technol., 23, 655–658 (2007).
[7] A. Beauger, J.C. Mutin and J.C. Niepce, J. Mater. Sci., 18, 3543–3550 (1983).
[8] J.C. Niepce and G. Thomas, Solid State Ionics, 43, 69–76 (1990).
[9] T. Kozawa, A. Onda and A. Yanagisawa, J. Eur. Ceram. Soc., 29, 3259–3264 (2009).
[10] C. Gomez-Yanez, C. Benitez and H. Balmori-Ramirez, Ceram. Int., 26, 271–277 (2000).
[11] L.B. Kong, J. Ma, H. Huang, R.F. Zhang and W.X. Que, J. Alloys Compd., 337, 226–230 (2002).
[12] R. Yanagawa, M. Senna, C. Ando, H. Chazono and J. Kishi, J. Am. Ceram. Soc., 90, 809–814 (2007).
[13] Y.B. Khollam, A.S. Deshpande, H.S. Potdar, S.B. Deshpande, S.K. Date and A.J. Patil, Mater. Lett., 55, 175–181 (2005).
[14] J.-D. Tsay, T.-T. Fang, T.A. Gubiotti and J.Y. Ying, J. Mater. Sci., 33, 3721–3727 (1998).
[15] S. Yoon, S. Baik, G.M. Kim and S. Namsoo, J. Am. Ceram. Soc., 89, 1816–1821 (2006).
[16] J. Azadmanjiri, H.K. Salehani, A. Dehghan-Hamedan and M. Sadeghi, Solid State Phenom., 121–123, 53–56 (2007).
[17] J.H. Park and S.D. Park, J. Chem. Eng. Jpn., 41, 631–638 (2008).
[18] X. Zhu, Z. Zhang, J. Zhu, S. Zhou and L. Liu, J. Cryst. Growth, 311, 2437–2442 (2009).
[19] P.K. Dutta and J.R. Gregg, Chem. Mater., 4, 843–846 (1992).
[20] M. Rössel, H.-R. Höche, H.S. Leipner, D. Völtzke, H.-P. Abicht, O. Hollricher, J. Müller and S. Gablenz, Anal. Bioanal. Chem., 280, 157–162 (2004).
[21] M. Rössel, S. Gablenz, T. Müller, A. Röder and H.-P. Abicht, Anal. Bioanal. Chem., 375, 310–314 (2003).
[22] S. Gablenz, C. Damm, F.W. Müller, G. Israel, M. Rössel, A. Roder and H.-P. Abicht, Solid State Sci., 3, 291–299 (2001).
[23] C.-Y. Chang, C.-Y. Huang, Y.-C. Wu, C.-Y. Su and C.-L. Huang, J. Alloys Compd., 495, 108–112 (2010).
[24] C.-Y. Chang, Doctoral dissertation, Department of Resources Engineering, National Cheng Kung University, Taiwan (2007).
[25] Y. Suyama and A. Kato, Bull. Chem. Soc. Jpn., 50, 1361–1366 (1977).
[26] H. Eguchi, Masters dissertation, Faculty of Engineering and Resource Science, Akita University, Japan (2012).
[27] M.T. Buscaglia, V. Buscaglia and R. Alessio, Chem. Mater., 19, 711–718 (2007).
[28] M.T. Buscaglia, V. Buscaglia, M. Viviani, G. Dondero, S. Röhrig, A. Rüdiger and P. Nanni, Nanotechnology, 19, 225602 (2008).
[29] R. Alessio, V. Buscaglia, M.T. Buscaglia, US 2008/0038181 A1 (2008).
[30] H. Miura, J. Crystallogr. Soc. Jpn., 45, 145–147 (2003).
[31] T. Kubo and K. Shinriki, J. Soc. Chem. Ind. Jpn., 54, 268–270 (1951).
[32] H. Nakamura, Y.-F. Chen, K. Kimura, H. Tateyama and H. Hirosue, J. Ceram. Soc. Jpn., 105, 1037–1041 (1997).
[33] K. Honda and T. Yoshikawa, Bunseki Kagaku, 56, 51–54 (2007).
[34] T. Kubo, M. Kato and T. Fujita, J. Soc. Chem. Ind. Jpn., 80, 847–853 (1967).
[35] Y. Fujikawa, F. Yamane and T. Nomura, J. Jpn. Soc. Powder Powder Metall., 50, 751–756 (2003).